Check for updates

Low-complexity sparse absolute-term based nonlinear equalizer for C-band IM/DD systems

JUNWEI ZHANG,[1,2] **ZHENRUI LIN,**[1] **XIONG WU,**[2] **JIE LIU,**[1] **ALAN PAK TAO LAU,**[3] **CHANGJIAN GUO,**[2,4,*] **CHAO LU,**[2] **AND SIYUAN YU**[1,5]

[1]*State Key Laboratory of Optoelectronic Materials and Technologies, School of Electronics and Information Technology, Sun Yat-Sen University, Guangzhou 510006, China*
[2]*Photonics Research Center, Department of Electronic and Information Engineering, The Hong Kong Polytechnic University, Hong Kong SAR, China*
[3]*Photonics Research Center, Department of Electrical Engineering, The Hong Kong Polytechnic University, Hong Kong*
[4]*South China Academy of Advanced Optoelectronics, South China Normal University, Guangzhou 510006, China*
[5]*Photonics Group, Merchant Venturers School of Engineering, University of Bristol, Bristol BS8 1UB, UK*
*changjian.guo@coer-scnu.org

Abstract: A low-complexity sparse absolute-term based nonlinear equalizer (AT-NLE) is proposed to eliminate the nonlinear signal distortions for intensity modulation and direct detection (IM/DD) systems. By performing the orthogonal matching pursuit (OMP) algorithm to adaptively obtain the significant kernels of both the linear and absolute terms, the computational complexity of the proposed sparse AT-NLE is dramatically reduced and independent of the memory length. The performance of the proposed sparse AT-NLE is experimentally evaluated in a C-band 56-Gbit/s four-level pulse-amplitude modulation (PAM-4) system over a 30-km standard single-mode fiber (SSMF). Experimental results show that compared with the conventional diagonally-pruned Volterra nonlinear equalizer (DP-VNLE) or DP-AT-NLE, the proposed sparse AT-NLE saves 77.7% or 76% real-valued multiplications when their achieved bit error ratios (BERs) are similar. Meanwhile, the proposed sparse AT-NLE reduces the computational complexity by $> 28\%$ compared to the sparse DP-VNLE at a BER of 5×10^{-4}. The proposed low-complexity sparse AT-NLE shows great potential for high-performance and low-cost IM/DD optical transmission systems.

1. Introduction

To support the proliferation of data traffic in optical data center interconnections and access networks, while meeting the demand of low-cost, energy-efficiency, and small form factors, intensity modulation and direct detection (IM/DD) systems have attracted significant attention [1–4]. Compared with conventional on-off keying (OOK) modulation systems, IM/DD systems based on advanced modulation formats such as discrete multi-tone (DMT), carrier-less amplitude phase (CAP) and four-level pulse-amplitude modulation (PAM-4) have been investigated extensively in recent years due to their higher spectrally efficiency [3,4]. Among them, PAM-4 can offer better balanced performance and computational complexity and has been chosen as a standard format in 400G Ethernet [5,6].

Nevertheless, the IM/DD transmission systems operating in C band are sensitive to the chromatic dispersion (CD) as well as modulation and detection related nonlinearity [7–18]. The modulation nonlinearity is dominant for multi-carrier DMT signals with high peak-to-average power ratio (PAPR) [7,8]. For PAM based transmission systems, the signal distortions are mainly resulted from the square-law detection related nonlinearity, which causes signal-to-signal beating

interference (SSBI) (i.e., 2nd-order nonlinear distortion) and power fading to the received signals [9,10]. The CD also enhances the time-dispersive effect of the nonlinear distortions. In order to improve the transmission performance, many digital signal processing (DSP) based nonlinear compensation techniques have been proposed to code with these nonlinear distortions in IM/DD systems [7–18].

One of the most popular approaches to compensate the nonlinearity in IM/DD systems is to use digital nonlinear equalizers (NLEs) based on well-known Volterra series [19,20], due to their abilities to model the complex time-dispersive nonlinear channel response. However, along with their superior performance comes high computational complexity, which grows exponentially as the channel memory length increases. This may limit their feasibility in cost-sensitive IM/DD optical communication systems. To address the computational complexity in Volterra NLEs (VNLEs), straightforward strategies are to prune some negligible beating terms [10–18]. By pruning the nonlinear terms with large delays, a 2nd-order diagonally-pruned VNLE (DP-VNLE) [10] or a polynomial nonlinear equalizer (PNLE) [10,11] with only the main diagonal terms have been investigated and demonstrated in IM/DD systems. To prune more negligible linear and nonlinear terms and further reduce the complexity, sparse VNLEs based on threshold pruning [12], L1- regularization [13], combination of L1- and L2- regularizations [14], and orthogonal matching pursuit (OMP) greedy algorithm [15] have been proposed and implemented in IM/DD transmission systems. To balance the performance and computational complexity, low-complexity frequency domain nonlinear equalizers have also been proposed in IM/DD systems [7,8].

Recently, the absolute terms $|x(n)|x(n)$ and $|x(n)|x^2(n)$ have been added to VNLE. The resultant ABS-based VNLE outperforms conventional VNLE in IM/DD systems, at the expense of increased computational complexity [16]. In [17] and [18], the absolute terms $|x(n) + x(n - q)|$ and $|x(n)|$ were adopted to replace the nonlinear terms $x(n)x(n - q)$ and $x^2(n)$ of conventional DP-VNLE and PNLE, respectively. Compared with conventional DP-VNLEs, these DP- absolute-term based NLEs (DP-AT-NLEs) save 20 ~ 40% real-valued multiplications at 7% hard-decision forward error correction (HD-FEC) limit [17,18]. However, the DP-AT-NLEs require a larger nonlinear memory length (i.e., relatively larger number of kernels) to achieve comparable performances compared to the DP-VNLE, which may also result in increased complexity.

In this paper, in order to further reduce the implementation complexity and improve the performance of nonlinear equalization, we propose a sparse AT-NLE to eliminate the nonlinear signal distortions for IM/DD systems. An OMP algorithm [21,22] is utilized to adaptively obtain the significant kernels of both linear and absolute terms of the sparse AT-NLE. The computational complexity can be dramatically reduced by controlling the sparsity level, which is independent of the memory length. We show that the required number of real-valued multiplications (RNRM) of the proposed sparse AT-NLE is the same as the number of significant kernels. Therefore, the complexity of the proposed sparse AT-NLE is significantly lower than those of DP-VNLE, DP-AT-NLE and sparse DP-VNLE. The performance of the proposed sparse AT-NLE is experimentally evaluated in a C-band 56-Gbit/s PAM-4 system over 30-km of standard single-mode fiber (SSMF). Experimental results show that compared with DP-VNLE or DP-AT-NLE, the proposed sparse AT-NLE saves the RNRM by 77.7% or 76% when their bit error ratios (BERs) are similar. Meanwhile, the proposed sparse AT-NLE can also save more than 28% of RNRM compared with that of sparse DP-VNLE at a BER of 5×10^{-4}. Therefore, the proposed low-complexity sparse AT-NLE shows a great potential in high-performance and low-cost IM/DD optical transmission systems.

2. Principle and computational complexity of the proposed sparse nonlinear equalizer

2.1. 2nd-order DP-VNLE and DP-AT-NLE

To effectively mitigate the linear and nonlinear transmission distortions in IM/DD systems, the DP-VNLE can be implemented as a post-equalizer at the receiver side. The nth sample of the output of the 2nd-order DP-VNLE can be expressed as [17]

$$y(n) = \sum_{k=0}^{N_1-1} w_1(k)x(n-k) + \sum_{q=0}^{Q-1} \sum_{k=0}^{N_2-1-q} w_2(k,q)x(n-k)x(n-k-q) \tag{1}$$

where $x(n)$ is the nth sample of the received signal corrupted by linear and nonlinear distortions, w_k and N_k are the mth-order ($m = 1, 2$) kernel and memory length of the DP-VNLE, respectively. Q is the pruning factor, which is used to prune the unimportant cross-beating terms composed of received signals at larger delays in time. The DP-VNLE becomes the VNLE or PNLE when $Q = N_2$ or $Q = 1$, respectively.

By replacing the cross-beating terms in DP-VNLE with the terms formed of the absolute value of a sum of two input samples, the 2nd-order DP-AT-NLE can be written as [17]

$$y(n) = \sum_{k=0}^{N_1-1} w_1(k)x(n-k) + \sum_{q=0}^{Q-1} \sum_{k=0}^{N_2-1-q} w_2(k,q)|x(n-k) + x(n-k-q)| \tag{2}$$

where $|\bullet|$ donates the absolute operator. Applying the Taylor series expansion of $|x|$ at $x = 0$, $|x| \approx x^2/2 - x^4/8$ can be obtained. Thus the $|x(n) + x(n-q)|$ not only contains the nonlinear terms $x(n)x(n-q)$ in DP-VNLE, but also reduces the order of the NLE by one. The absolute operation can be realized by an addition [23] instead of a multiplication, and thus reduce the computational complexity.

2.2. Proposed sparse AT-NLE

We rewrite the DP-AT-NLE of Eq. (2) as

$$y(n) = \sum_{l=0}^{L-1} h_l x_l(n) \tag{3}$$

where h_l is the kernel with a size of $L = N_1+Q(2N_2-Q+1)/2$, $x_l(n)$ is the linear or absolute terms (i.e., $x(n-k)$ or $|x(n-k) + x(n-k-q)|$) . In training process, the kernels in Eq. (3) can be obtained using training sequence. For using M-point training sequence, we can rewrite the input-output relationship of Eq. (3) in a matrix form as:

$$\mathbf{y} = \sum_{l=0}^{L-1} h_l \mathbf{x}_l = \mathbf{X}\mathbf{h} \tag{4}$$

where $\mathbf{y} = [y(0), y(2), \cdots y(M-1)]^T$ is the transmitted training vector, $\mathbf{X}$ and $\mathbf{h}$ are $M{\times}L$ measurement matrix and $L{\times}1$ kernel vector, respectively, defining as

$$\mathbf{X} = [\mathbf{x}_0, \mathbf{x}_1, \cdots \mathbf{x}_{L-1}] \tag{5}$$

$$\mathbf{x}_l = [x_l(0), x_l(1), \cdots x_l(M-1)]^T \tag{6}$$

$$\mathbf{h} = [h_0, h_1, \cdots h_{L-1}]^T \tag{7}$$

where $(\bullet)^T$ stands for transposition. The kernels in Eq. (3) can be obtained based on the least squares (LS) algorithm [24]:

$$\mathbf{h} = (\mathbf{X}^H\mathbf{X})^{-1}\mathbf{X}^H\mathbf{y} \tag{8}$$

where $(\bullet)^H$ and $(\bullet)^{-1}$ stand for conjugate transposition and matrix inversion, respectively.

Since the linear and nonlinear responses of the IM/DD transmission systems are sparse [12–15], it is feasible to only use the most significant kernels while discarding the unimportant ones. To further reduce the computational complexity of nonlinear equalization, here we propose a low-complexity sparse AT-NLE, which can be expressed as

$$y(n) = \sum_{p=0}^{P-1} h'_p x'_p(n) \tag{9}$$

where h'_p and $x'_p(n)$ are the kernels and input signal terms of the proposed sparse AT-NLE, respectively, P is the sparsity level as well as the total number of kernels. The kernels of the sparse AT-NLE can be obtained in the training process using orthogonal matching pursuit (OMP) greedy algorithm [21,22], which adaptively searches for a good approximation of the transmitted training vector $\mathbf{y}$ in the linear combination of a small number of columns from the measurement matrix $\mathbf{X}$. The detailed procedures of OMP based kernel estimation are summarized as:

1) Initialize the residual $\mathbf{b}_0 = \mathbf{y}$, the index set $\mathbf{\Lambda}_0 = \phi$, the matrix of chosen atoms $\mathbf{S}_0 = \phi$, and the iteration counter $p = 1$.

2) Find the index $k_p = \arg\max_l |\mathbf{x}_l^H \mathbf{b}_{p-1}|$, where $l = 0, 1, \cdots, L-1$ and $l \notin \mathbf{\Lambda}_{p-1}$.

3) Augment the index set $\mathbf{\Lambda}_p = \mathbf{\Lambda}_{p-1} \cup k_p$ and the matrix of chosen atoms $\mathbf{S}_p = [\mathbf{S}_{p-1}, \mathbf{x}_{k_p}]$.

4) Solve the least squares (LS) problem $\mathbf{h}'_p = (\mathbf{S}_p^H \mathbf{S}_p)^{-1} \mathbf{S}_p^H \mathbf{y}$ and update the new residual $\mathbf{b}_p = \mathbf{y} - \mathbf{S}_p \mathbf{h}'_p$.

5) If $p < P$, $p = p + 1$ and return to Step 2.

6) The optimal index set $\mathbf{\Lambda} = \mathbf{\Lambda}_P$ and kernels $\mathbf{h}' = [h'_0, h'_1, \cdots h'_{P-1}]^T$ are obtained.

Figures 1(a) and 1(b) show the schematic diagrams of the DP-AT-NLE and the proposed sparse AT-NLE in equalization process, respectively. Compared with DP-AT-NLE, the received distorted signals can be equalized by using the sparse AT-NLE with much fewer kernel coefficients.
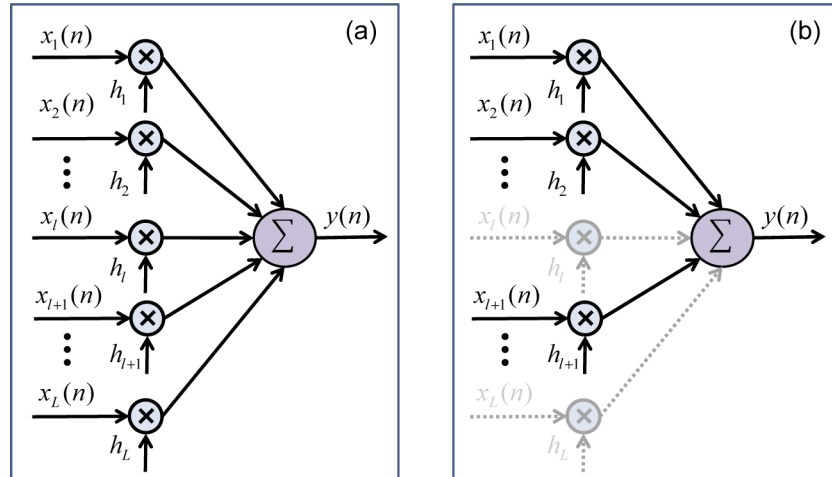

Fig. 1. Schematic diagrams of the (a) DP-AT-NLE and (b) sparse AT-NLE.

2.3. Complexity analysis

The computational complexity of the equalizer, which is strongly correlated to the power consumption, is one of the most significant factors for its real application. The proposed sparse AT-NLE is quantified by the number of real-valued multiplications. In the training process, $M(L\text{-}p)$ real-valued multiplications are required to obtain the index k_p in step 2, while $O(p^3)+(M+1)p^2+Mp$ and Mp real-valued multiplications are required for the LS algorithm and update of new residual in step 4, respectively. Since the fiber channel is quasi-invariant in IM/DD systems, the training process is not necessary once the kernel coefficients of the equalizers are estimated [17,18]. In addition, the sparse kernel coefficients can be further updated by the LS algorithm with the known optimal index set, which reduces the computational complexity from $O(L^3)+(M+1)L^2+ML$ to $O(P^3)+(M+1)P^2+MP$ compared to the DP-AT-NLE. Therefore, we mainly consider the computational complexity of equalizer in equalization process. Thanks to kernel reduction and absolute operation, the proposed sparse AT-NLE needs only P $(P < L)$ real-valued multiplications regardless of the memory length, which is much lower than that of the conventional DP-VNLE and DP-AT-NLE, in which $N_1+Q(2N_2\text{-}Q+1)$ and $N_1+Q(2N_2\text{-}Q+1)/2$ real-valued multiplications are required, respectively [17]. Moreover, the computational complexity of the proposed sparse AT-NLE is also lower than that of the sparse DP-VNLE, which requires $C_1+2(P\text{-}C_1)$ real-valued multiplications, where C_1 is the number of significant linear kernels in sparse DP-VNLE. The detailed analyses of equalization performance and complexity among the proposed sparse AT-NLE, DP-VNLE, DP-AT-NLE and sparse DP-VNLE will be presented in section 4.

3. Experimental setup

The performance of the proposed sparse AT-NLE is evaluated in a C-band 56-Gbit/s PAM-4 based transmission system. The experimental setup and DSP block diagram are illustrated in Fig. 2. At the transmitter, 28-GBaud Gray-coded PAM-4 symbols are generated by an arbitrary waveform generator (AWG, Keysight M8195A) with 3-dB bandwidth of 20 GHz operating at a sample rate of 56-GSa/s. After that, the 28-GBaud PAM-4 electrical signal from AWG is amplified by linear electrical amplifiers (SHF S807) and then fed into a Mach-Zehnder modulator (MZM, Thorlabs LN05S-FC) for double side-band (DSB) electrical-optical conversion. The optical source is generated from a distributed feedback (DFB) laser with a center wavelength of 1550.12 nm. The output voltage of the AWG and the bias voltage of the MZM are first optimized and set to be 75 mV and 1 V, respectively. After 30-km SSMF transmission without any dispersion compensation, a variable optical attenuator (VOA) is employed to adjust the received optical power (ROP) of the received signal, which is then detected by using a 20-GHz photo detector (PD, DSC-R401HG). Finally, the detected electrical PAM-4 signal is analog-to-digital converted
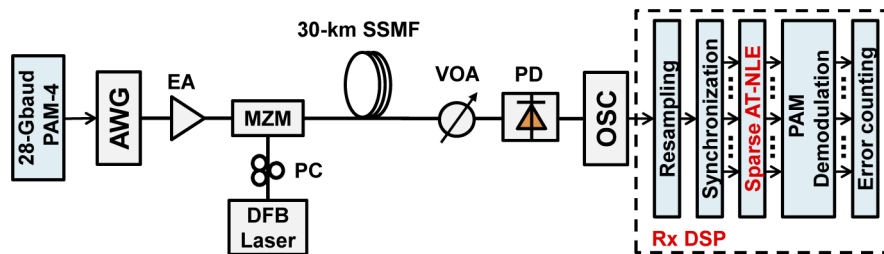
Fig. 2. Experimental setup of 56-Gb/s PAM-4 IM/DD system using sparse AT-NLE. AWG: arbitrary waveform generator; EA: electrical amplifier; MZM: Mach-Zehnder modulator; DFB: distributed feedback; PC: polarization controller; SSMF: standard single-mode fiber; VOA: variable optical attenuator; PD: photo detector; OSC: real-time oscilloscope.

at a real-time oscilloscope (OSC, DSA73304D) operating at a sample rate of 100 GSa/s. Finally, off-line DSP procedures including resampling, synchronization, half-symbol-spaced equalization with the proposed sparse AT-NLE, PAM demodulation and error counting are performed. In the training process, we use 10000 training symbols to obtain the kernel coefficients of the sparse AT-NLE, which remain unchanged in the equalization process. The BERs are evaluated by more than 2^{19} PAM-4 symbols.

4. Results and analysis

We first optimize the parameters including memory length, pruning factor and sparsity level of the nonlinear equalizers in an IM/DD PAM-4 based transmission system over 30-km SSMF at a ROP of 0 dBm. Figure 3(a) shows the measured BER versus the linear memory length N_1 for linear feedforward equalizer (FFE) (i.e., the linear part of the abovementioned NLEs). One can see that the BER performance of the FFE is improved as the memory length N_1 increases. The improvement becomes negligible when the memory length N_1 is no less than 30. Then we optimize the nonlinear memory length N_2 for the 2nd-order VNLE and AT-NLE with N_1 fixed to 30. The measured BER as a function of the nonlinear memory length N_2 is shown in Fig. 3(b). Compared with FFE, the BERs of VNLE and AT-NLE are significantly reduced. Besides, the performance of the AT-NLE is slightly worse than that of VNLE as expected [17]. For both VNLE and AT-NLE, saturated BER performance can be achieved when their nonlinear memory lengths N_2 is no less than 28. To balance the performance and complexity, $N_2 = 28$ is chosen for both VNLE and AT-NLE. Finally, we optimize the pruning factors Q of the DP-VNLE and DP-AT-NLE. The measured BER as a function of the pruning factor Q for the DP-VNLE and DP-AT-NLE is shown in Fig. 3(c). The BER performance is improved with a larger pruning factor and saturates at $Q = 9$. Thus, we set $Q = 9$ for the DP-VNLE and DP-AT-NLE in our experiment. For concision, (N_1, N_2, Q) denotes the parameters of the DP-VNLE and DP-AT-NLE in the experiment.

Different from the optimization of the conventional DP-VNLE and DP-AT-NLE, only the sparsity level P of the proposed sparse AT-NLE has impact on the computational complexity in nonlinear equalization. In addition, the OMP greedy algorithm can adaptively search for the significant kernels at a given search range of (N_1, N_2, Q) in training process. Thus, we optimize the sparsity level P of the proposed AT-NLE at different search ranges. The measured results are presented in Fig. 3(d). To meet the low-cost IM/DD application, we limit the sparsity level P of the proposed sparse AT-NLE to be less than 200. It can be seen that from Fig. 3(d): 1) The BER is significant reduced when utilizing a larger sparsity level. 2) The equalization performance can be further improved by employing a larger search range for the significant kernels. 3) The BER performance of the proposed sparse AT-NLE is better than that of the conventional DP-VNLE and DP-AT-NLE when the sparsity level P is larger than 100 and the search range is larger than (120, 120, 9). 4) The search range is optimized to be (150, 150, 9) in the experiment since the BER improvement is negligible when adopting a larger search range.

The equalization complexity of the proposed sparse AT-NLE is evaluated and compared with the conventional DP-VNLE and DP-AT-NLE after 30-km SSMF at a ROP of 0 dBm. The RNRM of the proposed sparse AT-NLE is the same as the value of the sparsity level P, while the complexity curves of the conventional DP-VNLE and DP-AT-NLE are obtained by varying the nonlinear memory length N_2 with $N_1 = 30$. Figures 4(a), 4(b), 4(c) and 4(d) show the measured BER as a function of RNRM for DP-VNLE and DP-AT-NLE when the pruning factor Q is set to be 3, 5, 7 and 9, respectively. The complexity curve of the proposed sparse AT-NLE with a search range of (150, 150, 9) is also included in Figs. 4(a)–4(d). The following observations could be made from Figs. 4(a)–4(d): 1) Similar as the results presented in Fig. 7 in [17], the DP-AT-NLE reduces the computational complexity when its performance is comparable to the conventional DP-VNLE in the low-complexity regions with a relatively small pruning factor Q.
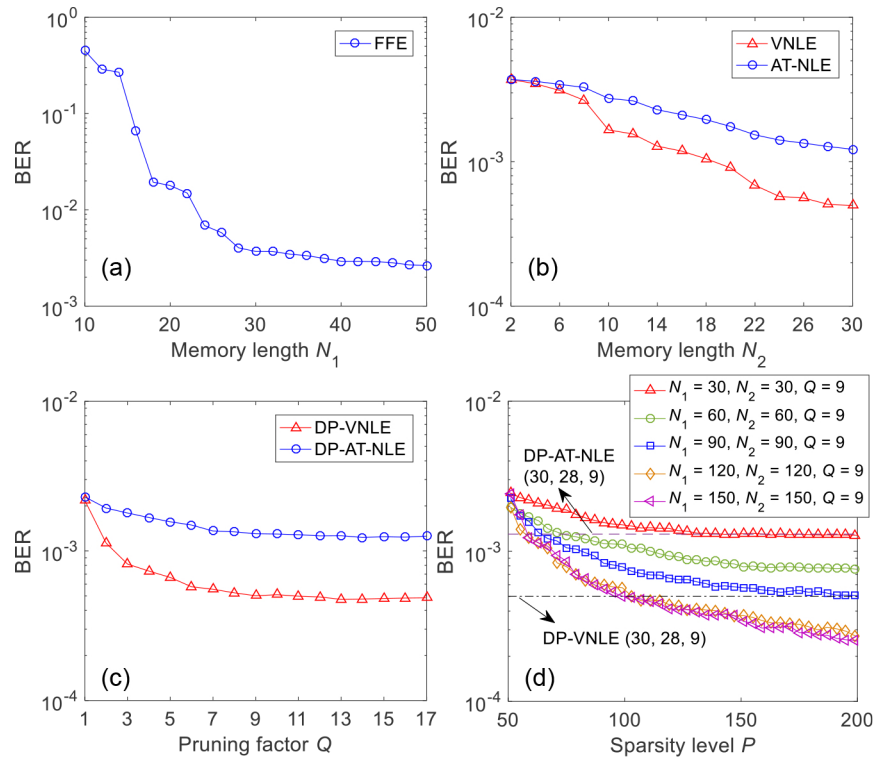
Fig. 3. (a) Measured BER versus memory length N_1 for linear FFE; (b) measured BER versus memory length N_2 for VNLE and AT-NLE with $N_1 = 30$; (c) measured BER versus pruning factor Q for DP-VNLE and DP-AT-NLE with $N_1 = 30$ and $N_2 = 28$; (d) measured BER versus sparsity level P for sparse AT-NLE. All results are measured after 30-km SSMF at a ROP of 0 dBm.

2) Meanwhile, the performance of the DP-AT-NLE underperforms the conventional DP-VNLE in the high complexity regions. 3) The results show that the proposed sparse AT-NLE significantly outperforms the conventional DP-VNLE and DP-AT-NLE in both of computational complexity and equalization performance, regardless of the nonlinear memory length N_2 and the pruning factor Q. 4) To achieve the similar BER performance of the conventional DP-VNLE (30, 28, 9) and DP-AT-NLE (30, 28, 9), the proposed sparse AT-NLE only requires 103 and 59 real-valued multiplications, which are 77.7% and 76% lower than 462 and 246 real-valued multiplications of DP-VNLE and DP-AT-NLE, respectively. 5) The BER can be further reduced from 5×10^{-4} to 2.6×10^{-4} by using the proposed sparse AT-NLE when switching from $P = 103$ to $P = 199$. In this case, the proposed sparse AT-NLE saves 56.9% real-valued multiplications and achieves better BER performance compared to the DP-VNLE (30, 28, 9).

The performance and complexity comparisons between the proposed sparse AT-NLE and sparse DP-VNLE are also evaluated after 30-km SSMF at a ROP of 0 dBm. The measured BER as a function of RNRM for different search ranges are presented in Figs. 5(a)–5(e). It can be summarized as follows: 1) The results show that the proposed sparse AT-NLE is a good choice for low-complexity application since the proposed sparse AT-NLE always outperforms the sparse DP-VNLE when the RNRM is less than 115 regardless of the search ranges. 2) In the cases of similar equalization complexity, the achieved BER performance of proposed sparse AT-NLE is much better than that of sparse DP-VNLE before the intersection point of the two compared complexity curves, which is extended when employing a larger search range. 3) To achieve the
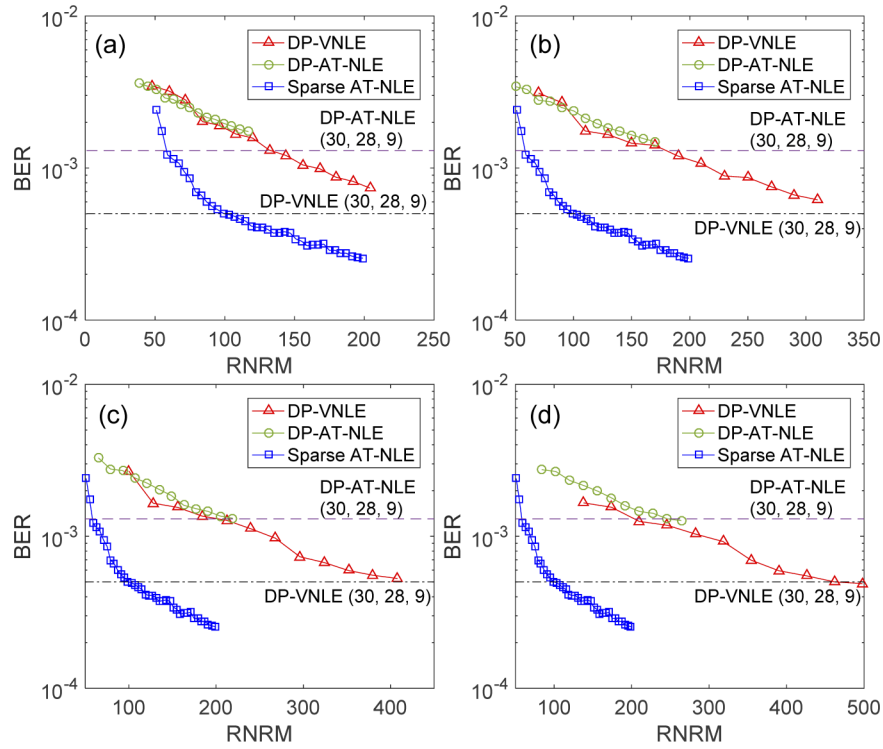
Fig. 4. Measured BER as a function of RNRM when (a) $Q = 3$, (b) $Q = 5$, (c) $Q = 7$ and (d) $Q = 9$. All results are measured after 30-km SSMF at a ROP of 0 dBm.

similar BER of 5×10^{-4} as the DP-VNLE (30, 28, 9), the proposed sparse AT-NLE at $P = 107$ and 103 lowers the RNRM by a factor of 31.1% and 28.8% compared to the sparse DP-VNLE with search ranges of (120, 120, 9) and (150, 150, 9), respectively. 4) The equalization performance of proposed sparse AT-NLE outperforms the sparse DP-VNLE with a search range of (150, 150, 9) when their real-valued multiplications are similar and below 200.

Finally, we evaluate the system transmission performance based on the proposed sparse AT-NLE. Figure 6(a) shows the measured BER versus the ROP for 56-Gbit/s PAM-4 signal transmission over 30-km SSMF. The results of the linear FFE, DP-VNLE (30, 28, 9) and DP-AT-NLE (30, 28, 9) are depicted for comparison. It can be seen that the liner FFE cannot reach the 7% HD-FEC limit of 3.8×10^{-3} when the ROP is less than 0 dBm. Compared with linear FFE, > 3 dB, ~ 3dB and > 2 dB improvement of the receiver sensitivity can be achieved by the proposed sparse AT-NLE, DP-VNLE and DP-AT-NLE, respectively. Note that the receiver sensitivity can be further improved by utilizing higher-bandwidth components or a higher-sensitivity receiver. In addition to significant complexity reduction, the performance of the proposed sparse AT-NLE with $P = 103$, 119 or 199 is slightly better than the DP-VNLE at 7% HD-FEC limit of 3.8×10^{-3}. To clearly show the performance improvement after using the proposed sparse AT-NLE, the corresponding received sequence diagrams for FFE, DP-VNLE, DP-AT-NLE and sparse AT-NLE with $P = 103$, 119 or 199 at a ROP of 0 dBm after 30-km SSMF transmission are shown in Figs. 6(b) to 6(g), respectively.
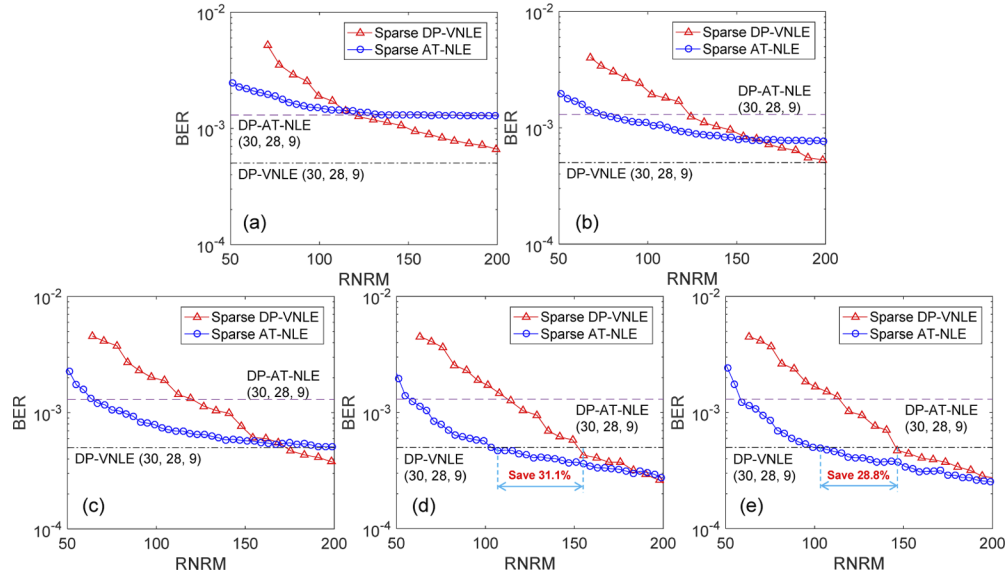
Fig. 5. Measured BER as a function of RNRM for different search ranges of (a) (30, 30, 9), (b) (60, 60, 9), (c) (90, 90, 9), (d) (120, 120, 9) and (e) (150, 150, 9). All results are measured after 30-km SSMF at a ROP of 0 dBm.
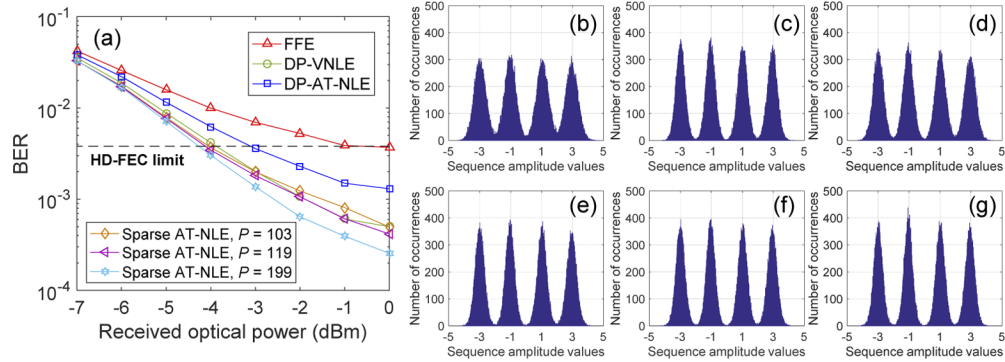
Fig. 6. (a) Measured BER versus ROP after 30-km SSMF transmission; received histograms for (b) FFE, (c) DP-VNLE, (d) DP-AT-NLE and sparse AT-NLEs with (e) $P = 103$, (f) $P = 119$ and (g) $P = 199$ at a ROP of 0 dBm.

5. Conclusion

We have proposed and experimentally demonstrated a low-complexity sparse AT-NLE to eliminate nonlinear signal distortions in IM/DD systems. By performing OMP algorithm to adaptively select the significant kernels of both the linear and absolute terms, the computational complexity of the proposed sparse AT-NLE is dramatically reduced and independent of the memory length. We have experimentally evaluated the equalization performance of the proposed sparse AT-NLE in a C-band 56-Gbit/s PAM-4 system over 30-km SSMF. Experimentally results show that compared with the conventional DP-VNLE, DP-AT-NLE and sparse DP-VNLE, the proposed sparse AT-NLE saves 77.7%, 76% and >28% real-valued multiplications, respectively, when their achieved BERs are similar. These results show that the proposed low-complexity sparse

AT-NLE has a great potential in high-performance and low-cost IM/DD optical transmission systems.

Disclosures. The authors declare no conflicts of interest.

Data availability. Data underlying the results presented in this paper are not publicly available at this time but may be obtained from the authors upon reasonable request.

References

1. M. Chagnon, "Optical communications for short reach," J. Lightwave Technol. **37**(8), 1779–1797 (2019).
2. Q. Hu, M. Chagnon, K. Schuh, F. Buchali, and H. Bülow, "IM/DD Beyond Bandwidth Limitation for Data Center Optical Interconnects," J. Lightwave Technol. **37**(19), 4940–4946 (2019).
3. K. Zhong, X. Zhou, J. Huo, C. Yu, C. Lu, and A. P. T. Lau, "Digital signal processing for short-reach optical communications: a review of current technologies and future trends," J. Lightwave Technol. **36**(2), 377–400 (2018).
4. J. Wei, T. Rahman, S. Calabrò, N. Stojanovic, L. Zhang, C. S. Xie, Z. C. Ye, and M. Kuschnerov, "Experimental demonstration of advanced modulation formats for data center networks on 200 Gb/s lane rate IMDD links," Opt. Express **28**(23), 35240–35250 (2020).
5. IEEE 802.3bs-2017 - IEEE Standard for Ethernet Amendment 10: Media Access Control Parameters, Physical Layers, and Management Parameters for 200 Gb/s and 400 Gb/s Operation.
6. J. Wei, Q. Cheng, R. V. Penty, I. H. White, and D. G. Cunningham, "400 Gigabit Ethernet Using Advanced Modulation Formats: Performance, Complexity, and Power Dissipation," IEEE Commun. Mag. **53**(2), 182–189 (2015).
7. J. Zhang, C. Guo, J. Liu, X. Wu, A. P. T. Lau, C. Lu, and S. Yu, "Low Complexity Frequency-Domain Nonlinear Equalization for 40-Gb/s/wavelength Long-Reach PON," in *Proc. OFC* 2018, paper W1J.8.
8. J. Zhang, C. Guo, J. Liu, X. Wu, A. P. Lau, C. Lu, and S. Yu, "Decision-Feedback Frequency-Domain Volterra Nonlinear Equalizer for IM/DD OFDM Long-Reach PON," J. Lightwave Technol. **37**(13), 3333–3342 (2019).
9. C. C. Wei, H. L. Chen, H. Y. Chen, Y. C. Chen, H. H. Chu, K. C. Chang, I. C. Lu, and J. Chen, "Analysis of nonlinear distortion and SSII cancellation in EAM-Based IMDD OFDM transmission," J. Lightwave Technol. **33**(14), 3069–3082 (2015).
10. N.-P. Diamantopoulos, H. Nishi, W. Kobayashi, K. Takeda, T. Kakitsuka, and S. Matsuo, "On the Complexity Reduction of the Second-Order Volterra Nonlinear Equalizer for IM/DD Systems," J. Lightwave Technol. **37**(4), 1214–1224 (2019).
11. J. Zhou, H. Wang, J. Wei, L. Liu, X. Huang, S. Gao, W. Liu, J. Li, C. Yu, and Z. Li, "Adaptive moment estimation for polynomial nonlinear equalizer in PAM8-based optical interconnects," Opt. Express **27**(22), 32210–32216 (2019).
12. J. Zhang, Y. Zheng, X. Hong, and C. Guo, "Increase in capacity of an IM/DD OFDM-PON using super-nyquist image induced aliasing and simplified nonlinear equalization," J. Lightwave Technol. **35**(19), 4105–4113 (2017).
13. W.-J. Huang, W.-F. Chang, C.-C. Wei, J.-J. Liu, Y.-C. Chen, K.-L. Chi, C.-L. Wang, J.-W. Shi, and J. Chen, "93% complexity reduction of Volterra nonlinear equalizer by ℓ 1-regularization for 112-Gbps PAM-4 850-nm VCSEL optical interconnect," in *Proc. OFC* 2018, Paper. M2D.7.
14. G. s. Yadav, C.-Y. Chuang, K.-M. Feng, J.-H. Yan, J. Chen, and Y.-K. Chen, "Reducing computation complexity by using elastic net regularization based pruned Volterra equalization in a 80 Gbps PAM-4 signal for inter-data center interconnects," Opt. Express **28**(26), 38539–38552 (2020).
15. J. Zhang, C. Guo, J. Liu, X. Wu, A. P. T. Lau, C. Lu, and S. Yu, "Orthogonal Matching Pursuit based Sparse Nonlinear Equalization for 40-Gb/s/wavelength Long-Reach PON," in *Proc. CLEO-PR* 2018, paper W2I.6.
16. L. Zhang, J Wei, N. Stojanovic, C. Prodaniuc, and C. Xie, "Beyond 200-Gb/s DMT transmission over 2-km SMF based on a low-cost architecture with single-wavelength, single-DAC/ADC and single-PD," in *Proc. ECOC* 2018, paper We1H.1.
17. Y. Yu, T. Bo, Y. Che, D. Kim, and H. Kim, "Low-complexity nonlinear equalizer based on absolute operation for C-band IM/DD systems," Opt. Express **28**(13), 19617–19628 (2020).
18. Y. Yu, M. R. Choi, T. Bo, Y. Che, D. Kim, and H. Kim, "Nonlinear equalizer based on absolute operation for IM/DD system using DML," IEEE Photonics Technol. Lett. **32**(7), 426–429 (2020).
19. E. Batista and R. Seara, "On the performance of adaptive pruned Volterra filters," Signal Process. **93**(7), 1909–1920 (2013).
20. J. Tsimbinos and K. V. Lever, "Computational complexity of Volterra based nonlinear compensators," Electron. Lett. **32**(9), 852–854 (1996).
21. J. Tropp and A. C. Gilbert, "Signal recovery from random measurements via orthogonal matching pursuit," IEEE Trans. Inf. Theory **53**(12), 4655–4666 (2007).

22. G. Z. Karabulut and A. Yongacoglu, "Sparse Channel Estimation using Orthogonal Matching Pursuit Algorithm," in *Proc. Vehicular Technol. Conference* 2014, 3880–3884.
23. S. Chen, "An area/time-efficient motion estimation micro core," IEEE Trans. Consum. Electron. **39**(3), 298–303 (1993).
24. A. Zaknich, *Principles of Adaptive Filters and Self-Learning Systems*, Springer, Berlin, Germany, 2006.